P4.8 PERFORMANCE OF A NEW VELOCITY DEALIASING ALGORITHM FOR THE WSR-88D

Arthur Witt* and Rodger A. Brown

NOAA/National Severe Storms Laboratory, Norman, Oklahoma

Zhongqi Jing

NOAA/National Weather Service Radar Operations Center, Norman, Oklahoma

1. INTRODUCTION

Improving the quality of the base velocity data in the WSR-88D is an ongoing effort (Crum et al. 1998). Although the current velocity dealiasing algorithm (VDA) in the WSR-88D Radar Product Generator (RPG) generally performs well, this is not always the case. In particular, when the WSR-88D is operating in Volume Coverage Pattern (VCP) – 31 (the low-Nyquist clear-air mode; Federal Meteorological Handbook, Number 11, Part A 2009), and wind speeds or vertical wind shear are high, there are often numerous velocity dealiasing errors. This causes many WSR-88D sites to instead primarily operate in VCP-32 (the high-Nyquist clear-air mode), despite the greater sensitivity of VCP-31 at detecting clear-air return. Even when the WSR-88D is operating at higher Nyquist velocities, instances of strong localized horizontal wind shear (e.g., mesocyclones, gust-fronts, etc.) can lead to frequent velocity dealiasing errors.

Given the limited computer capacity that existed when the WSR-88D was initially fielded (in 1989, for the prototype radar KOUN), its algorithms needed to be kept relatively computationally simple (i.e., they could not use large amounts of memory and/or CPU). Since then, substantial upgrades to the WSR-88D's computer systems allow for the implementation of more sophisticated algorithms, including a proposed new VDA.

The performance of the new VDA was compared to the current WSR-88D VDA, using a quantitative scoring procedure, on several recent VCP-31 cases where the current algorithm performed very poorly (i.e., it generated numerous/extensive errors). The performance comparison was also done for several convective-storm and hurricane events, where the WSR-88D was operating in two of the most commonly used precipitation-based VCPs.

*Corresponding author address: Arthur Witt, NSSL, 120 David L. Boren Blvd., Norman, OK 73072. E-mail: Arthur.Witt@noaa.gov

2. METHODS

The current VDA in the RPG is based on the method presented in Eilts and Smith (1990), including checks involving a vertical wind profile updated via the Velocity Azimuth Display (VAD) algorithm. For this project, the default adaptable parameter settings were used. Test cases were started without a manually entered initial vertical wind profile. Hence, the vertical wind profile was generated solely from the VAD algorithm.

The new VDA evaluated here is based on the two dimensional (2D) dealiasing algorithm (Algorithm A) described in section 2 of Jing and Weiner (1993). The technique attempts to dealias a connected 2D region on an elevation scan by minimizing all detected discontinuities due to aliasing. The algorithm uses a conventional threshold method, and discontinuity minimization is performed by solving a least-squares problem. A weighting factor has been added to the difference function of Equation (5) in Jing and Weiner (1993) for each border between two gates. The weighting depends on the difference between the two neighboring gates. If the difference is near zero or $2V_n$, the largest weighting is applied. As the difference increases, the weighting decreases. When the difference is near V_n, zero weighting is applied. This reduces/eliminates the contribution of noisy (unreliable) data to the optimization setting. With this improvement, the solutions of Equation (6) are mostly very close to $2kV_n$, where k is any integer. Gates that are not close to $2kV_n$ are considered aliased, and are dealiased by a simple environmental wind-based dealiasing algorithm. Thus, the histogram analysis described in Jing and Weiner (1993) is no longer needed.

In order to maximize the 2D performance (i.e., minimize dealiasing errors), we must apply the procedure to the entire elevation scan. Because the computing resources (CPU and memory) are often not sufficient to do this, we instead adopt a

two-phase dealiasing approach. In the first phase, we apply the 2D algorithm to the entire elevation scan, with sub-sampling of the data, if necessary (sub-sampling the data is a way to reduce the number of gates in a connected region before applying the 2D algorithm). This is done to obtain a reliable global wind distribution. In the second phase, we partition the elevation scan, and apply the 2D algorithm to each partition without sub-sampling. This allows for small features (e.g., tornadic vortex signatures) to be correctly dealiased. To determine the proper Nyquist velocity interval of small, isolated data regions, we use either an internally generated (via VAD analysis) environmental wind profile, or obtain the environmental wind from an external source (e.g., numerical model data, manually entered rawinsonde data, etc.). For the evaluation done here, the environmental wind profile was internally generated.

The performance of the new VDA was compared to the current WSR-88D VDA using data collected during three different instances when a WSR-88D site was operating in VCP-31. The three VCP-31 test cases selected (Table 1) were chosen because the current VDA performed very poorly (i.e., it generated numerous/extensive dealiasing errors; e.g., Fig. 1). The performance comparison was also done on two convective storm events (both from KTLX) and one hurricane case (from KLIX), when the WSR-88D site was operating in either of the two most commonly used precipitation-based scanning strategies (VCP-12 or VCP-212).

Base velocity data files (in netCDF format) were generated for both dealiasing algorithms using a specialized, off-line version of Build-11 of the WSR-88D RPG. Although only ~1 hour of data was used for the algorithm comparison in each test case, each RPG "run" was started earlier (usually several hours before the beginning of the comparison time period) in order to allow for the VAD-generated vertical wind profile in the RPG to become fully established. Since the base velocity data for all of the test cases where collected after the installation of Build-10 of the RPG, both legacy resolution (1.0° x 250 m) and "super" resolution (0.5° x 250 m) data (for elevation angles up to 1.5°) were available for comparison (Vogel et al. 2009). NSSL's WDSS-II display (Lakshmanan et al. 2007) was used to view and analyze the base velocity data files.

The scoring procedure was quantitative in nature and similar to that used in several other recent projects evaluating the accuracy of WSR-88D velocity dealiasing (Brown and Wood 2005; Witt 2007a,b). Each elevation scan analyzed was given an initial score of 100, and "points" were subtracted for each dealiasing error observed (Table 2). In difficult situations where it was not obvious whether or not an error had occurred, or what the correct solution was, then no points were subtracted (for that particular area of the elevation scan). Although the maximum penalty for a single error was –50 points, there was no limit on the number of separate errors that could be tabulated for the entire elevation scan. Hence, numerous small errors could ultimately add up to a sizable penalty.

3. TEST RESULTS

Based on the scoring methodology presented above, the new VDA consistently outperformed the current VDA (Table 3). The performance improvement of the new VDA was substantially greater for the VCP-31 cases versus the VCP-12/212 cases. This performance difference between the two VCP groups may be due to a combination of the much lower Nyquist velocities for the VCP-31 cases (11-12 m s^{-1}) versus the VCP-12/212 cases (mainly 25-34 m s^{-1}), and the deliberate selection of VCP-31 cases with extensive dealiasing errors for the current VDA (e.g., Fig. 2). The VCP-12/212 cases, on the other hand, were selected to represent more "typical" instances of dealiasing errors for the current VDA. Looking at performance as a function of elevation angle (Tables 4 and 5), performance scores for both algorithms are worst at the lowest elevation angle, and generally improve with increasing elevation angle. This is likely due to a combination of the larger amount of velocity data that potentially needs to be dealiased at the lower angles, along with the higher frequency of strong horizontal wind shear regions (e.g., mesocyclones, frontal boundaries, etc.).

4. DISCUSSION AND CONCLUSIONS

The test results for this project indicate that the new VDA offers the potential for improved dealiasing of the base velocity data, particularly when the WSR-88D is operating in VCP-31. However, even though the new VDA performed substantially better overall (in a relative sense) versus the current VDA on the three VCP-31 cases, it still had considerable difficulty properly dealiasing the lowest elevation scan, which is usually considered by end users of the velocity data to be the most important elevation scan (in the full set of elevation scans within a VCP). One

important factor unique to these VCP-31 test cases was the presence of a frontal boundary near the radar site. As the radar beam scanned through the boundary on the lowest elevation scan, the location of the abrupt wind shift associated with the front was not always readily apparent in the velocity data. For some portions of the scan, there was very little gradient in the velocity field where the boundary was located. However, the boundary location was apparent in the spectrum width data (as regions of high spectrum width). Hence, any VDA relying solely on gradients in the velocity data to perform its dealiasing will have great difficulty properly handling this situation. One possible solution for this problem would be to remove the velocity data associated with high spectrum width regions prior to dealiasing. This probably would be wise in any case, as this high spectrum-width data do not appear to be of any practical use, since the data are of dubious accuracy, and the velocities can't be made to match the environmental wind field. However, should this additional step be adopted in the dealiasing process, it would likely be necessary to restrict its use to weather situations not involving important severe storm signatures (e.g., mesocyclones, tornadic vortex signatures). Another option would be to have the VDA utilize both the velocity and spectrum width data in its dealiasing process.

Beyond its clearly superior performance for the VCP-31 cases, the new VDA also consistently outperformed the current VDA for the VCP-12/212 cases, although the amount of improvement was small due to the modest degree of dealiasing errors for the current VDA. Because the data set used in this project was quite small (only ~6 hours in total for all the test cases combined), more extensive testing is necessary before one can confidently recommend replacing the current VDA with the new VDA described here. However, these initial performance results are very promising, and indicate the potential, in the near future, for improvements in the quality of the WSR-88D velocity data, particularly for the now seldom-used VCP-31.

5. ACKNOWLEDGMENTS

The authors thank Travis Smith for reviewing the manuscript. This project was supported by the NEXRAD Radar Operations Center.

6. REFERENCES

Brown, R., and V. Wood, 2005: Evaluation of the Velocity Dealiasing Algorithm modified for super-resolution WSR-88D data. Final Report for the FY 2005 NSSL-ROC MOU (Task 5.1), 13pp. [Available from the NEXRAD Radar Operations Center.]

Crum, T. D., R. E. Saffle, and J. W. Wilson, 1998: An update on the NEXRAD program and future WSR-88D support to operations. *Wea. Forecasting,* **13**, 253-262.

Eilts, M. D., and S. D. Smith, 1990: Efficient dealiasing of Doppler velocities using local environmental constraints. *J. Atmos. Oceanic Technol..* **7,** 118-128.

Federal Meteorological Handbook, Number 11, Part A (2009): System concepts, responsibilities, and procedures. FCM-H11A-2009, Federal Coordinator for Meteorological Services and Supporting Research. Available online at: http://www.ofcm.gov/fmh11/fmh11parta/pdf/2009-PartA_FMH11.pdf

Jing, Z., and G. Weiner, 1993: Two-dimensional dealiasing of Doppler velocities. *J. Atmos. Oceanic Technol..* **10,** 798-808.

Lakshmanan, V., T. Smith, G. J. Stumpf, and K. Hondl, 2007: The warning decision support system – integrated information (WDSS-II). *Wea. Forecasting,* **22**, 592-608.

Vogel, J. M., C. Payne, C. A. Van Den Broeke, and L. R. Lemon, 2009: Impacts of super-resolution data on National Weather Service warning decision making. Available online at: http://www.caps.ou.edu/reu/reu09/papers/Vogel.pdf

Witt, A., 2007a: Performance of two velocity dealiasing algorithms on Terminal Doppler Weather Radar data. *Preprints,* 33rd Conference on Radar Meteorology, Cairns, Australia, American Meteorological Society, CD-ROM, P13A.14.

Witt, A., 2007b: Final report on the FY 2007 NSSL-ROC MOU Task 8: Velocity Dealiasing, 14pp. [Available from the NEXRAD Radar Operations Center.]

Table 1. List of the test cases. All times are in UTC, and the date corresponds to the start time. Acronyms: VCP = Volume Coverage Pattern; LP = Light precipitation; FB = frontal boundary; SL = Squall-line.

Radar site	Date	Analysis period Start Time	End Time	VCP	Weather situation
KDMX	03 Dec 2008	13:04	14:01	31	LP with FB
KTLX	16 Dec 2008	11:58	12:54	31	FB
KTLX	26 Jan 2009	22:48	23:44	31	LP with FB
KLIX	01 Sep 2008	16:03	17:15	212	Hurricane
KTLX	23 Mar 2009	23:39	00:42	12	SL with supercells
KTLX	12 Apr 2009	05:31	06:26	12	Thunderstorms

Table 2. Penalties for the different types of dealiasing errors.

Description of Error	Penalty
Single gate or 2 adjacent gates	–1
Small radial spike (<3 km in length)	–2
Very small patch	–2 to –3
Small patch	–4 to –8
Large patch	–8 to –12
Swath of ~20°	–12 to –16
Swath of ~40°	–26 to –30
Swath of ~60°	–32 to –38
Swath of ~90° or larger	–40 to –50

Table 3. Average performance scores for the current and new VDA for each test case. Acronyms: LR = legacy resolution; SR = super resolution.

Date	All elevation scans		LR elevation scans		SR elevation scans	
	Current	New	Current	New	Current	New
03 Dec 2008	24.5	57.3	47.1	70.5	–32.0	24.2
16 Dec 2008	62.5	85.7	72.7	87.6	37.0	81.1
26 Jan 2009	1.5	75.0	42.4	82.2	–100.8	57.0
01 Sep 2008	94.6	99.98	95.7	99.97	89.4	100
23 Mar 2009	97.8	99.7	98.5	99.8	94.4	99.4
12 Apr 2009	98.7	99.9	98.7	99.9	95.4	99.0

Table 4. Average performance scores for each elevation angle for the VCP-31 test cases.

Elevation	LR scans		SR scans	
Angle	Current	New	Current	New
0.5°	–22.4	30.1	–64.6	27.6
1.5°	21.7	77.7	0.8	80.6
2.5°	83.6	97.5		
3.5°	94.0	98.8		
4.5°	93.5	96.3		

Table 5. Average performance scores for each elevation angle for the VCP-12/212 test cases.

Elevation	LR scans		SR scans	
Angle	Current	New	Current	New
0.5°	91.2	99.2	92.1	99.1
0.9°	93.8	99.4	92.6	99.7
1.3°	93.3	99.8	94.5	99.5
1.8°	93.2	100		
2.4°	97.3	100		
3.1°	99.1	100		
4.0°	99.9	99.97		
5.1°	99.97	100		
6.4°	99.97	100		
8.0°	100	100		
10.0°	100	100		
12.5°	99.97	100		
15.6°	99.97	100		
19.5°	99.6	100		

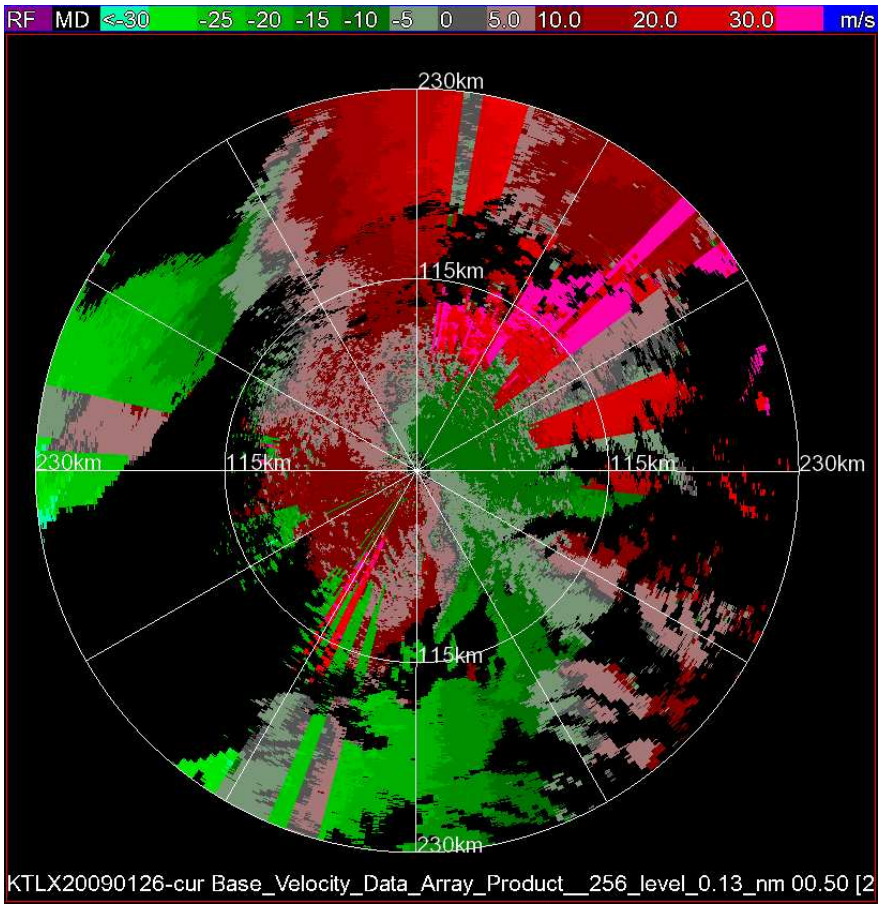

Fig. 1. Example of velocity dealiasing errors from the current WSR-88D VDA. The data shown come from the KTLX 0.5° elevation scan on 26 Jan 2009 at 23:07:24 UTC.

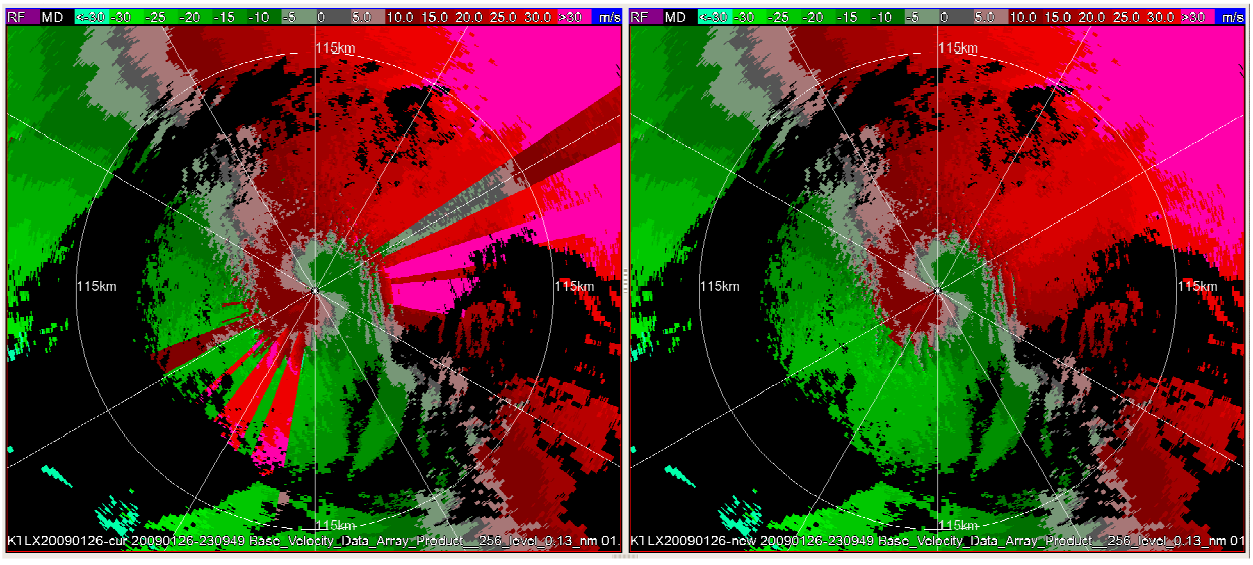

Fig. 2. Example of the differences in velocity dealiasing from the current VDA (left) and new VDA (right). The data shown come from the KTLX 1.5° elevation scan on 26 Jan 2009 at 23:09:49 UTC.